Elastic scattering losses from colliding Bose-Einstein condensates

Paweł Ziń,[1] Jan Chwedeńczuk,[1] and Marek Trippenbach[1,2]
[1]*Institute for Theoretical Physics, Warsaw University, Hoża 69, PL-00-681 Warsaw, Poland*
[2]*Soltan Institute for Nuclear Studies, Hoża 69, PL-00-681 Warsaw, Poland*
(Received 5 December 2005; published 6 March 2006)

Bragg diffraction divides a Bose-Einstein condensate into two overlapping components, moving with respect to each other with high momentum. Elastic collisions between atoms from distinct wave packets can significantly deplete the condensate. Recently, Ziń *et al.* [Phys. Rev. Lett. **94**, 200401 (2005)] introduced a model of two counterpropagating atomic Gaussian wave packets incorporating the dynamics of the incoherent scattering processes. Here we study the properties of this model in detail, including the nature of the transition from spontaneous to stimulated scattering. Within the first-order approximation, we derive analytical expressions for the density matrix and anomalous density that provide excellent insight into correlation properties of scattered atoms.

DOI: 10.1103/PhysRevA.73.033602 PACS number(s): 03.75.Nt

I. INTRODUCTION

A light-induced potential applied to a Bose-Einstein condensate (BEC) can be used to make high momentum daughter BEC wave packets, which propagate through the parent condensate [1–3]. Such a technique has been used to make an atom laser [4], to study the coherence properties of condensates [3,5,6], and to study nonlinear four-wave mixing (4WM) of coherent matter waves [7–10]. In the process of a collision between two condensates, inevitably, some atoms would scatter away, forming often a noticeable halo around the region of collision. The halo at the level above noise indicates profuse elastic scattering losses, and has been observed in various experiments, for example, [2,11,12].

A scheme of such a process is illustrated in Fig. 1, where the collision of two condensates having mean wave vector $\pm Q$ is shown in the momentum space. The condensates are denoted by large dots and marked as $\psi_{\pm Q}$. Atoms from these two counterpropagating wave packets undergo elastic collisions and can be scattered out into all the modes permitted by the energy and momentum conservation (a pair of such states is marked with small dots). These modes lie within the three-dimensional shell, which in Fig. 1 is represented by the gray ring.

The elastic scattering loss is not accounted for by the Gross-Pitaevskii equation (GPE). Recently, some modifications of the GPE were proposed in order to incorporate this loss into the mean-field dynamics. This has been done either within the slowly varying envelope approximation by adding an imaginary part to the scattering length [13], or by including a stochastic component to mimic quantum field fluctuations [14,15]. Interesting results were also obtained using the method based on the field theory formulation in the lowest order of the perturbation approximation [16,17]. So as to test the validity of various approximate schemes, an exact (nonperturbative) model of collisional losses was proposed [18]. It is valid both in the regime of spontaneous initiation and Bose enhancement. This model assumes spherical nonspreading Gaussians for the colliding wave packets and is capable of treating the number of scattered atoms as well as their statistical properties through the higher-order correlation functions.

Here we study this model in more detail, including the nature of the transition from spontaneous to stimulated scattering and statistical properties of scattered atoms. We also provide a link to previous results obtained within the perturbation approximation.

II. THE MODEL

A system of bosons interacting via contact potential is described by the Hamiltonian

$$H = -\int d^3r \hat{\Psi}^\dagger(\mathbf{r},t)\frac{\hbar^2\nabla^2}{2m}\hat{\Psi}(\mathbf{r},t) + \frac{g}{2}\int d^3r \hat{\Psi}^\dagger(\mathbf{r},t)\hat{\Psi}^\dagger(\mathbf{r},t)\hat{\Psi}(\mathbf{r},t)\hat{\Psi}(\mathbf{r},t), \quad (1)$$

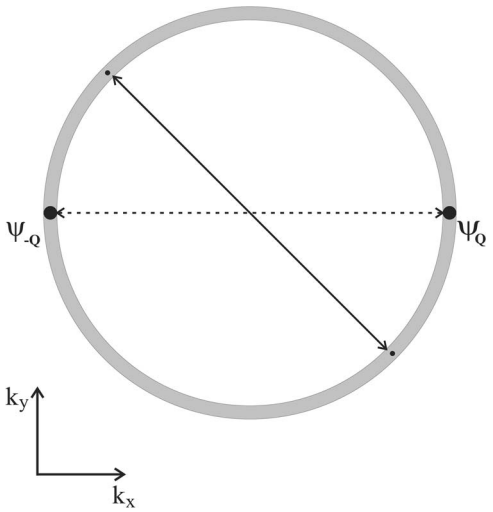

FIG. 1. Collision of condensates in momentum space. Big dots denoted as $\psi_{\pm Q}$ represent colliding condensates. Small dots represent scattered atoms. Dashed lines represent anihilation of atoms, solid lines represent creation of atoms; it should help to imagine the annihilation of two atoms, one from each of the condensates, and the creation of two atoms in such states, so that the momentum and energy of the system is conserved.

where $\hat{\Psi}(\mathbf{r},t)$ is a field operator satisfying equal time bosonic commutation relations, m is the atomic mass, and g determines the strength of the interatomic interactions. Since the Hamiltonian (1) is of the fourth order in $\hat{\Psi}$, the Heisenberg equation governing the evolution of the field,

$$i\hbar\,\partial_t\hat{\Psi}(\mathbf{r},t) = -\frac{\hbar^2\nabla^2}{2m}\hat{\Psi}(\mathbf{r},t) + g\hat{\Psi}^\dagger(\mathbf{r},t)\hat{\Psi}(\mathbf{r},t)\hat{\Psi}(\mathbf{r},t), \tag{2}$$

is nonlinear and thus, in general, analytically and numerically untractable. However, for some physical systems, a Bogoliubov approximation can be applied leading to linear Heisenberg equations. The idea underlying this approximation states that for some cases the field operator might be split into two parts: ψ and $\hat{\delta}$. The first contribution describes macroscopically occupied modes, where the fluctuations are usually small; hence its operator character might be dropped (ψ becomes a c-number wave function satisfying the GPE). The second part $\hat{\delta}$, called the "above mean field part," representing fluctuations, requires full quantum-mechanical treatment. Since the initial state of the system consists of two counterpropagating atomic wave packets and the "sea" of the unoccupied modes, the Bogoliubov approximation can be applied. The splitting of the bosonic field is performed in the following manner:

$$\hat{\Psi}(\mathbf{r},t) = \psi_Q(\mathbf{r},t) + \psi_{-Q}(\mathbf{r},t) + \hat{\delta}(\mathbf{r},t), \tag{3}$$

where the subscript $\pm Q$ denotes the mean momentum of the colliding condensates and $\psi_Q(\mathbf{r},t)+\psi_{-Q}(\mathbf{r},t)$ satisfies the time-dependent GPE. Upon inserting Eq. (3) into the Heisenberg equation (2), one obtains on the right-hand side several terms, of which, in the spirit of the Bogoliubov approximation, we keep only those up to the first order in $\hat{\delta}$,

$$\begin{aligned} i\hbar\,\partial_t\hat{\delta}(\mathbf{r},t) = &\Bigg[-\frac{\hbar^2\nabla^2}{2m} + 2g|\psi_Q(\mathbf{r},t)|^2 + 2g|\psi_{-Q}(\mathbf{r},t)|^2 \\ &+ 2g\psi_Q^*(\mathbf{r},t)\psi_{-Q}(\mathbf{r},t) \\ &+ 2g\psi_{-Q}^*(\mathbf{r},t)\psi_Q(\mathbf{r},t)\Bigg]\hat{\delta}(\mathbf{r},t) \\ &+ g[2\psi_Q(\mathbf{r},t)\psi_{-Q}(\mathbf{r},t) + \psi_Q^2(\mathbf{r},t) \\ &+ \psi_{-Q}^2(\mathbf{r},t)]\hat{\delta}^\dagger(\mathbf{r},t). \end{aligned} \tag{4}$$

The above equation can be simplified using the following arguments. First, we expect that for as long as the mean kinetic energy of the scattered atoms $\hbar^2Q^2/(2m)$ is much larger than the interaction energy (gn, where n is the mean density of the atoms in the condensate), the mean-field energy terms $[2g|\psi_Q(\mathbf{r},t)|^2+2g|\psi_{-Q}(\mathbf{r},t)|^2 + 2g\psi_Q^*(\mathbf{r},t)\psi_{-Q}(\mathbf{r},t)+2g\psi_{-Q}^*(\mathbf{r},t)\psi_Q(\mathbf{r},t)]$ can be dropped, leading to

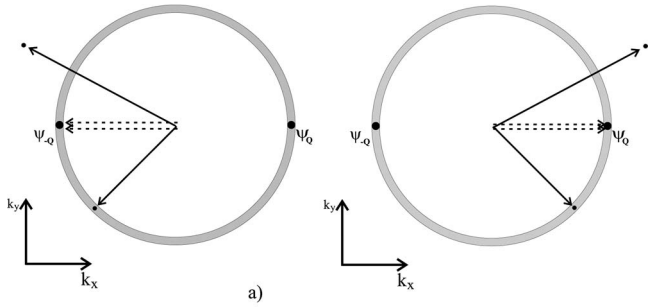

FIG. 2. Visualizations of the $g\hat{\delta}^\dagger(\mathbf{r},t)[\psi_Q^2(\mathbf{r},t)+\psi_{-Q}^2(\mathbf{r},t)]$ term. (a) represents the term proportional to ψ_{-Q}^2. Two atoms are annihilated from ψ_{-Q} and scattered to such states in which the momentum is conserved. Analogous plot (b) is a visualization of the term proportional to ψ_Q^2.

$$\begin{aligned} i\hbar\,\partial_t\hat{\delta}(\mathbf{r},t) = &-\frac{\hbar^2\nabla^2}{2m}\hat{\delta}(\mathbf{r},t) + g[2\psi_Q(\mathbf{r},t)\psi_{-Q}(\mathbf{r},t) + \psi_Q^2(\mathbf{r},t) \\ &+ \psi_{-Q}^2(\mathbf{r},t)]\hat{\delta}^\dagger(\mathbf{r},t). \end{aligned} \tag{5}$$

To make further simplifications more transparent, we visualize the effects of various terms in the momentum space using a schematic picture. The first term, $2g\hat{\delta}^\dagger(\mathbf{r},t)\psi_Q(\mathbf{r},t)\psi_{-Q}(\mathbf{r},t)$, is a source term. It corresponds to annihilation of two particles from counterpropagating condensates and creation of two particles in the field of the "sea" of scattered atoms. An example of such a process is illustrated in Fig. 1. The second term, $g\hat{\delta}^\dagger(\mathbf{r},t)[\psi_Q^2(\mathbf{r},t) + \psi_{-Q}^2(\mathbf{r},t)]$, as shown in Fig. 2, describes annihilation of a pair of particles from the same condensates (either ψ_Q or ψ_{-Q}) and creation of two particles in the $\hat{\delta}$ field. As seen from Fig. 2, this process is nonresonant, leading to violation of the conservation laws.

The above arguments imply that the Bogoliubov equation (5) can be simplified by dropping the off-resonant term and leaving only the source term. The evolution equation for the $\hat{\delta}$ field finally becomes

$$i\hbar\,\partial_t\hat{\delta}(\mathbf{r},t) = -\frac{\hbar^2\nabla^2}{2m}\hat{\delta}(\mathbf{r},t) + 2g\psi_Q(\mathbf{r},t)\psi_{-Q}(\mathbf{r},t)\hat{\delta}^\dagger(\mathbf{r},t). \tag{6}$$

To simplify the dynamics even further, we define and compare three characteristic time scales of the problem. Let σ and $N/2$ be the Thomas-Fermi radius and the number of particles in each of the colliding condensates. Then the collisional time (the time it takes for each wave packet to pass through its colliding partner) is defined by $t_C=(m\sigma)/(\hbar Q)$. Another characteristic time scale of the problem is the linear dispersion time (time of the spread of the wave packet due to kinetic energy term), $t_{\mathrm{LD}}=m\sigma^2/\hbar$ [9]. In the same manner, the nonlinear dispersion time, which is the time of ballistic expansion in the Thomas-Fermi approximation [19], can be defined: $t_{\mathrm{ND}}=\sqrt{\pi^{3/2}m\sigma^5/gN}$. The dynamics of the system depends on the relations between these time scales. It is convenient to introduce the following dimensionless parameters:

$t_{\mathrm{LD}}/t_C=\beta$ and $(t_{\mathrm{LD}}/t_{\mathrm{ND}})^2=\alpha$. When the number of elastically scattered atoms is small in comparison with the total number of atoms in both wave packets and both linear and nonlinear dispersion time scales are much longer than the collision time $[(t_{\mathrm{LD}}/t_C)=\beta\gg 1$ and $(t_{\mathrm{ND}}/t_C)^2=\beta^2/\alpha\gg 1]$, we can neglect the change in population and shape of the macroscopically occupied functions $\psi_{\pm Q}(\mathbf{r},t)$ during the collision. In our model, we assume a Gaussian shape of the colliding condensates

$$\psi_{\pm Q}(\mathbf{r},t)=\sqrt{\frac{N}{2\pi^{3/2}\sigma^3}}\exp\left[\pm iQx_1-\frac{i\hbar tQ^2}{2m}\right]\times\exp\left\{-\frac{1}{2\sigma^2}\left[\left(x_1\mp\frac{\hbar Qt}{m}\right)^2+x_2^2+x_3^2\right]\right\}, \quad (7)$$

where $\mathbf{r}=(x_1,x_2,x_3)$. We have chosen to approximate the condensate profile with the Gaussian function to make the problem analytically tractable and get a better insight into all relevant physical aspects of the system. The width of the Gaussian is chosen to match the width of the Thomas-Fermi radius.

Upon substituting Eq. (7) into Eq. (6), and then rescaling the variables $\mathbf{r}/\sigma\rightarrow\mathbf{r}$, we obtain

$$i\beta\partial_t\hat{\delta}(\mathbf{r},t)=-\frac{1}{2}\Delta\hat{\delta}(\mathbf{r},t)+\alpha e^{-r^2-t^2-i\beta t}\hat{\delta}^{\dagger}(\mathbf{r},t). \quad (8)$$

Next we switch to dimensionless field operators substituting $\hat{\delta}(\mathbf{r},t)\sigma^{3/2}\rightarrow\hat{\delta}(\mathbf{r},t)$. Notice that the assumption of spherical symmetry of the colliding wave packets imposes such symmetry on Eq. (8). Thus it is convenient to decompose $\hat{\delta}$ into the basis of spherical harmonics,

$$\hat{\delta}(\mathbf{r},t)=\sum_{n,l,m}R_{n,l}(r)Y_{lm}(\theta,\phi)\hat{a}_{n,l,m}(t), \quad (9)$$

where $\hat{a}_{n,l,m}$ are annihilation operators for a particle in the mode described by n,l,m quantum numbers. There is still a freedom of choice with regard to the set of orthogonal functions $R_{n,l}(r)$. As we shall see below, a good candidate is a set of eigenfunctions of spherically symmetric harmonic oscillators,

$$R_{n,l}(r)=\sqrt{\frac{2n!\,a_0^{-3}}{\Gamma\left(l+n+\frac{3}{2}\right)}}\left(\frac{r}{a_0}\right)^l e^{-r^2/2a_0^2}L_n^{l+(1/2)}\left(\frac{r^2}{a_0^2}\right), \quad (10)$$

where $L_n^{l+(1/2)}(x)$ is the associated Laguerre polynomial [20] and a_0, a harmonic-oscillator length, is an auxiliary free parameter that can be chosen to minimize the computational effort. Notice that the choice of orthogonal basis preserves bosonic commutation relations for annihilation and creation operators $a_{n,l,m}$,

$$[a_{n,l,m},a_{n'l'm'}^{\dagger}]=\delta_{nn'}\delta_{mm'}\delta_{ll'}, \quad (11)$$

$$[a_{n,l,m},a_{n'l'm'}]=0, \quad [a_{n,l,m}^{\dagger},a_{n'l'm'}^{\dagger}]=0. \quad (12)$$

Substituting Eq. (9) into Eq. (8) and making use of the completeness of the basis functions, we obtain the equation governing the evolution of operator $a_{n,l,m}$,

$$i\partial_t\hat{a}_{n,l,m}=B_{n,l}\hat{a}_{n,l,m}+D_{n,l}\hat{a}_{n-1,l,m}+D_{n+1,l}\hat{a}_{n+1,l,m}+\frac{\alpha}{\beta}e^{-t^2}\sum_{n'}C_{n,n',l}\hat{a}_{n',l,-m}^{\dagger}, \quad (13)$$

where $E_{n,l}=(2n+l+3/2)/a_0^2$, $B_{n,l}=(E_{n,l}-\beta^2)/2\beta$, $D_{n,l}=\sqrt{n(n+l+1/2)}/(2\beta a_0^2)$, and

$$C_{n,n',l}=\int_0^{\infty}r^2drR_{n,l}(r)\exp(-r^2)R_{n'l}(r)=\sqrt{\frac{\Gamma\left(n+l+\frac{3}{2}\right)\Gamma\left(n'+l+\frac{3}{2}\right)}{\Gamma\left(l+\frac{3}{2}\right)^2\Gamma(n+1)\Gamma(n'+1)}}(1+a_0^2)^{-l-(3/2)}\times\left[\frac{a_0^2}{1+a_0^2}\right]^{n+n'}F\left(-n,-n',l+\frac{3}{2},1/a_0^4\right). \quad (14)$$

Here $F(a,b,c,x)$ is a hypergeometric function [20]. Notice that all coupling coefficients are calculated analytically and the $\hat{a}_{n,l,m}$ operators for different l and m are decoupled. Moreover, Eqs. (13) do not depend on quantum number m. With all these simplifications, the linear system of Eqs. (13) can be solved numerically. The general three-dimensional problem, due to spherical symmetry, simplifies to the set of one-dimensional ordinary differential equations. In numerical applications, for every l a basis of approximately 64 modes associated with quantum number n is sufficient. Moreover, simulations show that 50 modes associated with quantum number l is usually enough. Thus the whole quantum model can be solved numerically on an ordinary PC within one hour of calculations.

We define a vector of operators,

$$\mathbf{v}_{l,m}(t)=\begin{pmatrix}\hat{a}_{0,l,m}\\ \hat{a}_{1,l,m}\\ \vdots\\ \hat{a}_{n_{max},l,m}\\ \hat{a}_{0,l,-m}^{\dagger}\\ \hat{a}_{1,l,-m}^{\dagger}\\ \vdots\\ \hat{a}_{n_{max},l,-m}^{\dagger}\end{pmatrix},$$

and rewrite Eq. (13) in the compact form

$$i\frac{d}{dt}\mathbf{v}_{l,m}(t)=\hat{\mathbf{A}}_l(t)\mathbf{v}_{l,m}(t). \quad (15)$$

The matrix $\hat{\mathbf{A}}_l(t)$ is plotted schematically in Fig. 3.

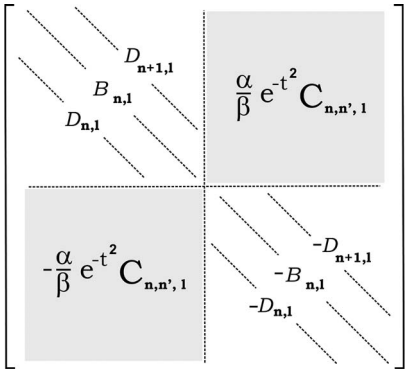

FIG. 3. Visualization of $\hat{\mathbf{A}}_l(t)$ matrix from Eq. (15). It is tridiagonal in coupling $a_{n,l,m}$'s with $a_{n',l,m}$'s and $a^{\dagger}_{n,l,-m}$'s with $a^{\dagger}_{n',l,-m}$'s. The coupling between $a_{n,l,m}$'s and $a^{\dagger}_{n',l,-m}$'s is determined by $-(\alpha/\beta)e^{-t^2}C_{n,n',l}$. In general, all $C_{n,n',l}$'s are nonzero, which is represented by the gray area.

The solution $\mathbf{v}_{l,m}(t)$ can be expressed in terms of the time evolution operator,

$$\mathbf{v}_{l,m}(t) = \hat{\mathbf{U}}_l(t)\mathbf{v}_{l,m}(0). \tag{16}$$

The evolution operator satisfies the equation

$$\frac{d\hat{\mathbf{U}}_l(t)}{dt} = -i\hat{\mathbf{A}}_l(t)\hat{\mathbf{U}}_l(t) \tag{17}$$

with the initial condition $\hat{\mathbf{U}}_l(0)=\mathbf{1}$. In our calculations, we evaluate $\hat{\mathbf{A}}_l(t)$ and find the evolution matrix $\hat{\mathbf{U}}_l(t)$ by solving Eq. (17). The matrix $\hat{\mathbf{U}}_l(t)$ uniquely determines full operator dynamics of $\hat{\delta}(\mathbf{r},t)$ and hence is sufficient to obtain any expectation value of the variables referring to the system.

Equation (8) can be treated alternatively in the Fourier domain. Upon defining the Fourier transform in the form

$$\hat{\delta}(\mathbf{r},t) = \left(\frac{\beta}{2\pi}\right)^{3/2} \int d^3k \exp(i\beta\mathbf{k}\mathbf{r} - i\beta k^2 t/2)\hat{\delta}(\mathbf{k},t),$$

we can rewrite Eq. (8) as

$$i\partial_t\hat{\delta}(\mathbf{k},t) = \frac{\alpha\beta^2}{8\pi^{3/2}}e^{-t^2}\int d^3k \exp\left(-\frac{\beta^2(\mathbf{k}+\mathbf{k}')^2}{4}\right) \times\exp\left[-i\beta t\left(1-\frac{k^2+k'^2}{2}\right)\right]\hat{\delta}^{\dagger}(\mathbf{k}',t). \tag{18}$$

We took this particular form of the Fourier transform (with factor β) so that the wave vector of the moving condensate is equal to unity.

III. FIRST-ORDER PERTURBATION THEORY

The advantage of using the Fourier transform lies in the fact that Eq. (18) can be used in a natural way as a basis of the perturbative expansion. Assuming a general solution of $\delta(\mathbf{k},t)$ in a perturbative form, $\delta(\mathbf{k},t)=\delta^{(0)}(\mathbf{k},t)+\delta^{(1)}(\mathbf{k},t)+\cdots$, we derive a recurrent relation, which in the lowest order gives

$$i\partial_t\hat{\delta}^{(1)}(\mathbf{k},t) = \frac{\alpha\beta^2}{8\pi^{3/2}}e^{-t^2}\int d^3k' \exp\left(-\frac{\beta^2(\mathbf{k}+\mathbf{k}')^2}{4}\right) \times\exp\left[-i\beta t\left(1-\frac{k^2+k'^2}{2}\right)\right]\hat{\delta}^{(0)\dagger}(\mathbf{k}',t). \tag{19}$$

The first-order equation (19) can be integrated and consequently we can evaluate observable quantities like the number of scattered atoms or the correlation functions analytically.

A. Density matrix

In this subsection, we find the approximate expression for the density matrix of scattered atoms,

$$\rho(\mathbf{k}_1,\mathbf{k}_2,t) = \langle\hat{\delta}^{\dagger}(\mathbf{k}_1,t)\hat{\delta}(\mathbf{k}_2,t)\rangle, \tag{20}$$

within the first-order perturbation theory. We perform the calculations in the momentum space.

Our system is initially in the vacuum state $|\Omega\rangle$, that is, $\hat{\delta}(\mathbf{k},0)|\Omega\rangle=0$. Hence, due to the commutation relation, $[\hat{\delta}(\mathbf{k},t),\hat{\delta}^{\dagger}(\mathbf{k}',t)]=\delta^3(\mathbf{k}-\mathbf{k}')$, at initial time we have

$$\langle\hat{\delta}(\mathbf{k},0)\hat{\delta}^{\dagger}(\mathbf{k}',0)\rangle = \delta^3(\mathbf{k}-\mathbf{k}'). \tag{21}$$

Then, upon substituting Eq. (19) into Eq. (20), and using Eq. (21), we obtain

$$\begin{aligned}\rho(\mathbf{k}_1,\mathbf{k}_2,t) = \frac{\alpha^2\beta^4}{64\pi^3}\int_0^t d\tau\int_0^t d\tau' \exp(-\tau^2-\tau'^2) \\ \times\exp\left(-\frac{\beta^2(k_1^2+k_2^2)}{4} - i\beta(\tau k_1^2 - \tau' k_2^2)/2\right) \\ \times\int d^3k \exp\left(-\frac{\beta^2[k^2+\mathbf{k}\cdot(\mathbf{k}_1+\mathbf{k}_2)]}{2}\right) \\ \times\exp[i\beta(\tau-\tau')(1-k^2/2)].\end{aligned} \tag{22}$$

We show how to handle the above integral in Appendix A. For $\beta\gg 1$ and $\beta|\mathbf{k}_1+\mathbf{k}_2|\gg 1$, the density matrix reduces to

$$\begin{aligned}\rho(\mathbf{k}_1,\mathbf{k}_2,t) = \frac{\alpha^2\beta\sqrt{2\pi}}{32\pi^2}\exp\left(-\frac{\beta^2|\mathbf{k}_1-\mathbf{k}_2|^2}{8}\right) \\ \times\int_0^t d\tau\int_0^t d\tau' \exp\left(-\frac{(\tau-\tau')^2|\mathbf{k}_1+\mathbf{k}_2|^2}{8}\right) \\ \times\exp\left[-\tau^2-\tau'^2+i\beta\tau\left(1-\frac{|\mathbf{k}_1+\mathbf{k}_2|^2}{8}-\frac{k_1^2}{2}\right)\right] \\ \times\exp\left[-i\beta\tau'\left(1-\frac{|\mathbf{k}_1+\mathbf{k}_2|^2}{8}-\frac{k_2^2}{2}\right)\right].\end{aligned} \tag{23}$$

This expression, although it still contains a twofold integral over time, is simple enough to give the distribution of scattered atoms, and provides a further insight into coherence properties and dynamics of the scattering process.

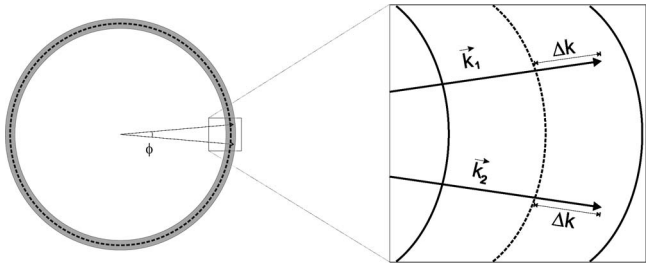

FIG. 4. Configuration of vectors $\mathbf{k}_1$ and $\mathbf{k}_2$ as in case (a). The vectors are of the same length, with angle ϕ between them. The dashed circle corresponds to $k=1$ and the gray area is the scattering shell. The length of each of the vectors differs from unity by Δk.

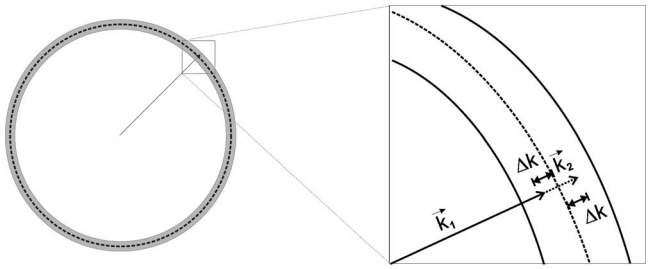

FIG. 5. Configuration of vectors $\mathbf{k}_1$ and $\mathbf{k}_2$ as in case (b). The vectors are parallel. The dashed circle corresponds to $k=1$ and the gray area is the scattering shell. The lengths of $\mathbf{k}_1$ and $\mathbf{k}_2$ differ from unity by $\pm\Delta k$.

B. Final momentum distribution and coherence properties of scattered atoms

From the last expression in the previous section [Eq. (23)], the density matrix becomes negligible if any of the arguments

$$\beta|\mathbf{k}_1-\mathbf{k}_2|,$$

$$\beta\left(1-\frac{|\mathbf{k}_1+\mathbf{k}_2|^2}{8}-\frac{k_2^2}{2}\right)$$

or

$$\beta\left(1-\frac{|\mathbf{k}_1+\mathbf{k}_2|^2}{8}-\frac{k_1^2}{2}\right),$$

appearing in the exponential functions, is large (remember that we work under the constant assumption $\beta\gg 1$). Hence the only regions where we expect a nonvanishing value of $\rho(\mathbf{k}_1,\mathbf{k}_2,t)$ are those for which wave vectors k_1 and k_2 are close to each other ($|\mathbf{k}_1-\mathbf{k}_2|\ll 1$), and they both have length close to unity (notice that in our units this coincides with the length of the wave vector of the colliding condensates). It is interesting to examine the following two cases.

(a) Equal length case: $k_1=k_2\equiv 1+\Delta k$. In this case (see Fig. 4), the vectors $\mathbf{k}_1$ and $\mathbf{k}_2$ are of equal length and form an angle ϕ. The properties of the density matrix strongly depend on the distance from the resonance surface Δk. For small values of Δk and small angles ϕ, the density matrix can be approximated by the Gaussian function

$$\rho(\Delta k,\phi)=\mathcal{A}\exp\left(-\frac{\beta^2\phi^2}{8}-\frac{\beta^2\Delta k^2}{2}\right). \tag{24}$$

The constant

$$\mathcal{A}=\frac{\alpha^2\beta}{128\sqrt{\pi}}\left[1+\frac{2}{\pi}\arctan\left(\frac{1}{2\sqrt{2}}\right)\right]$$

was found evaluating Eq. (23) analytically on resonance ($\mathbf{k}_1=\mathbf{k}_2$ and $|\mathbf{k}_1|=1$). Notice that Eq. (24) for $\phi=0$ represents the density of the cloud of scattered atoms. The cloud has spherical symmetry, following the symmetry of Eq. (8). It takes a form of a shell localized around $k=1$ (which corresponds to wave vector Q in our units). Its width is of order $1/\beta$.

(b) Parallel vectors case: $\mathbf{k}_1\|\mathbf{k}_2$ (see Fig. 5). Wave vectors are shifted away from the resonance in the opposite direction [$\mathbf{k}_1=\mathbf{e}(1-\Delta k)$ and $\mathbf{k}_2=\mathbf{e}(1+\Delta k)$]. In this case, we also find a Gaussian fit

$$\rho(\Delta k)=\mathcal{A}\exp\left(-\frac{2}{3}\beta^2\Delta k^2+i\beta\Delta k\right).$$

This concludes our analysis of the density matrix. Now we move on to the first-order correlation function

$$g_1(\mathbf{k}_1,\mathbf{k}_2,t)=\frac{\langle\hat{\delta}^\dagger(\mathbf{k}_1,t)\hat{\delta}(\mathbf{k}_2,t)\rangle}{\sqrt{\langle\hat{\delta}^\dagger(\mathbf{k}_1,t)\hat{\delta}(\mathbf{k}_1,t)\rangle\langle\hat{\delta}^\dagger(\mathbf{k}_2,t)\hat{\delta}(\mathbf{k}_2,t)\rangle}}. \tag{25}$$

We find that in the case (a),

$$g_1(\Delta k,\phi)=\exp\left(-\frac{\beta^2\phi^2}{8}\right), \tag{26}$$

while in the case (b),

$$g_1(\Delta k)=\exp\left(-\frac{1}{6}\beta^2\Delta k^2+i\beta\Delta k\right). \tag{27}$$

By comparing Eq. (27) describing the coherence in the radial direction, $g_1(\Delta k)$, and Eq. (24) describing the density $\rho(\Delta k,\phi=0)$, it seems reasonable to assume that the radial coherence length of the shell of scattered atoms is of the same order as its width. Following this observation, we present a very rough estimate of the number of atoms necessary for the bosonic stimulation to occur. First we introduce the concept of the coherence volume associated with each scattered atom. It is determined by the first-order correlation function. If we fix $\mathbf{k}_1$ and vary $\mathbf{k}_2$, we get a well-defined peaked structure around $\mathbf{k}_2=\mathbf{k}_1$. The size of this structure gives the coherence volume associated with the single atom (see Fig. 6). As we have already shown, the radial extent of this structure is of order of $1/\beta$. From Eq. (26), we deduce that the angular coherence length is of the same order $1/\beta$. Hence we estimate the coherence volume to be equal to $1/\beta^3$. Next we remind ourselves that the volume V in the momentum space accessible by the scattered atoms is a spherical shell determined by the diagonal part of the density matrix. In our case, $V=4\pi/3[1+1/(2\beta)]^3-4\pi/3[1-(1/2\beta)]^3\simeq 4\pi/\beta$. When the product of the number of scattered atoms times their coherence volume is comparable with V, the coherence volumes associated with distinct atoms start

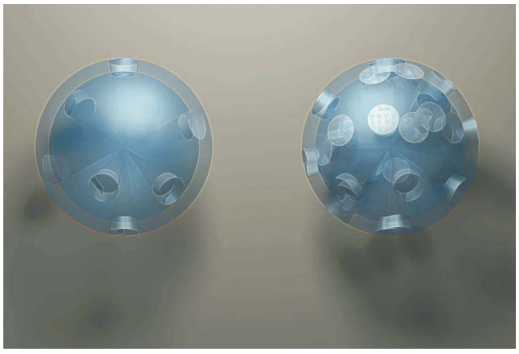

FIG. 6. (Color online) The artistic representation of the atomic coherence. Final states of scattered atoms lie on the spherical shell and the coherence volume of each atom is marked as a dark region in this shell. Case (a) corresponds to weak scattering, and in (b) individual coherence volumes start to overlap.

to overlap (see Fig. 6). Then, the wave nature of matter comes into play, and interference effects would enhance the scattering-bosonic stimulation [21]. Using the above estimates, the critical number of atoms is equal to $4\pi\beta^2$. In the next section, we derive a more practical criterion for bosonic stimulation to show up in the collision of the condensates.

C. Number of scattered atoms for $t \gg 1/\beta$

The most straightforward observable quantity, namely the number of scattered atoms as a function of time, can be expressed in terms of the trace of the density matrix,

$$\mathcal{S}(t) = \int d^3k \rho(\mathbf{k},\mathbf{k},t). \tag{28}$$

Using Eq. (23), we get

$$\mathcal{S}^{(1)}(t) = \frac{\alpha^2\beta}{4\sqrt{2\pi}} \int_0^\infty k^2 dk \int_0^t d\tau \int_0^t d\tau' \exp(-\tau^2 - \tau'^2) \times \exp\left(i\beta(1-k^2)(\tau-\tau') - \frac{k^2}{2}(\tau-\tau')^2 \right). \tag{29}$$

Unless k is close to unity, the integral over τ and τ' will vanish due to the rapidly oscillating phase factor $\beta(1-k^2) \times (\tau-\tau')$. Thus it is convenient to change the variables $k = 1 + (x/\beta)$ and expand the integrand in the lowest order of x obtaining

$$\mathcal{S}^{(1)}(t) = \frac{\alpha^2\sqrt{2\pi}}{8\pi} \int_{-\infty}^\infty dx \int_0^t d\tau \int_0^t d\tau' \exp(-\tau^2 - \tau'^2) \times \exp\left(i2x(\tau-\tau') - \frac{1}{2}(\tau-\tau')^2 \right). \tag{30}$$

Next, evaluating the integral over x, we get

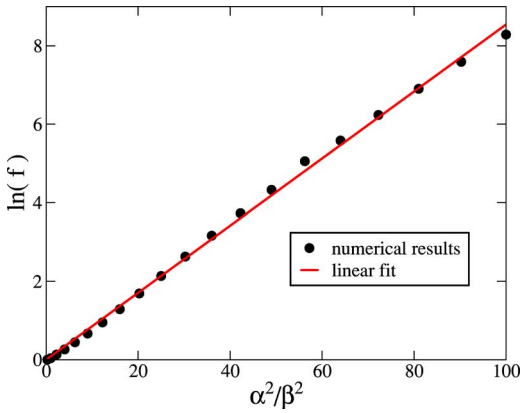

FIG. 7. (Color online) Elastic collision loss as a function of α^2/β^2. The total number of scattered atoms is given by $\mathcal{S} = \pi(\alpha^2/16) f(\alpha^2/\beta^2)$. The figure shows that $\ln(f)$ is a linear function of α^2/β^2 with slope equal to 0.085.

$$\mathcal{S}^{(1)}(t) = \frac{\alpha^2\sqrt{2\pi}}{8} \int_0^t d\tau \int_0^t d\tau' \, \delta(\tau-\tau') \times \exp\left(-\tau^2 - \tau'^2 - \frac{1}{2}(\tau-\tau')^2 \right), \tag{31}$$

and finally the number of scattered atoms is equal to

$$\mathcal{S}^{(1)}(t) = \frac{\pi\alpha^2}{16} \operatorname{erf}(t\sqrt{2}). \tag{32}$$

In Appendix B, the same result is obtained within a classical model of colliding hard spheres with cross section equal to $8\pi a^2$.

An important remark concerns the condition for bosonic stimulation. As we mentioned in the previous section, it occurs when $\mathcal{S} \geqslant 4\pi\beta^2$. By comparing this result with Eq. (32) (with $t \to \infty$), we get $\alpha/\beta \geqslant 2$. This is a simple condition, which, translated into experimental parameters, provides the criterion for bosonic enhancement in the collision of two condensates. To verify this condition, we evaluate the total number of scattered atoms up to the third order,

$$\mathcal{S}^{(1)} + \mathcal{S}^{(2)} + \mathcal{S}^{(3)} = \pi\frac{\alpha^2}{16}\left(1 + c_1\frac{\alpha^2}{\beta^2} + c_2\frac{\alpha^4}{\beta^4} \right), \tag{33}$$

where c_1 and c_2 are numerical coefficients. This suggests the functional dependence of the form $\mathcal{S} = \pi(\alpha^2/16) f(\alpha^2/\beta^2)$, where $f(0) = 1$. Our previous numerical results [18], obtained both in perturbative and nonperturbative regimes, confirm this suggestion. In Fig. 7, we plot the logarithm of f versus $(\alpha/\beta)^2$ and obtain a straight line with high accuracy. Hence we see that indeed the bosonic stimulation [manifested by the value of $f(\alpha^2/\beta^2)$ being larger than unity] occurs for $\alpha/\beta \approx 2$. Moreover, function f has an exponential form $f[(\alpha/\beta)^2] \simeq \exp[0.085(\alpha/\beta)^2]$. Using the above formulas, one can both easily estimate the number of scattered atoms and predict whether bosonic enhancement would be present in the particular physical realization.

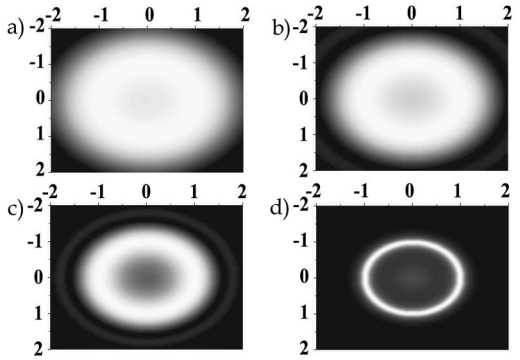

FIG. 8. The density of atoms in momentum space as given by Eq. (35) for $\alpha=10$ and $\beta=20$. The halo of scattered atoms shrinks, forming a shell around $k=1$. The four frames correspond to increasing times (a) $t=0.07t_c$, (b) $t=0.1t_c$, (c) $t=0.15t_c$, and (d) $t=0.4t_c$, where t_c is the collisional time.

D. Number of scattered atoms for $t \ll 1$. Characteristic time scales of the signal build up

In order to analyze the dynamics of $\langle \hat{\delta}^\dagger \hat{\delta} \rangle$ on a very short time scale, we consider the diagonal part of the density matrix

$$\rho(\mathbf{k},\mathbf{k},t) = \frac{\alpha^2\beta\sqrt{2\pi}}{32\pi^2}\int_0^t d\tau \int_0^t d\tau' \exp(-\tau^2-\tau'^2) \times \exp\left(-\frac{(\tau-\tau')^2k^2}{2} + i\beta(\tau-\tau')(1-k^2)\right). \tag{34}$$

Notice that for very short times ($t \ll 1$), all the terms proportional to the squares of τ and τ' in the exponents appearing in Eq. (34) can be dropped. With this simplification, the time integrals can be evaluated analytically, giving

$$\rho(\mathbf{k},\mathbf{k},t) = \frac{\alpha^2\beta\sqrt{2\pi}}{32\pi^2}\frac{\sin^2[\beta t(1-k^2)/2]}{[\beta(1-k^2)/2]^2}. \tag{35}$$

The time evolution of the density of scattered atoms in the k_x-k_y plane is pictured in Fig. 8. It shows that atoms, which initially scatter isotropically in the momentum space, eventually form a well pronounced halo around $k=1$.

To relate Eq. (35) to the number of scattered atoms, we need to perform the integration over $\mathbf{k}$. Evaluating the angular integral explicitly and changing the variables $x=\beta t(k^2-1)/2$, we get

$$S(t) = \frac{\alpha^2\sqrt{2\pi}}{8\pi}t\int_{-\beta t/2}^{\infty} dx \frac{\sin^2 x}{x^2}\sqrt{\frac{2x}{\beta t}+1}.$$

This formula can be further simplified in the following two regimes:

(a) $\beta t \ll 1$: we set the lower limit in the integral equal to zero and use the approximation $\sqrt{(2x/\beta t)+1} \simeq \sqrt{2x/\beta t}$ to obtain

$$S(t) \simeq \frac{\alpha^2\sqrt{2\pi}}{8\pi}t\sqrt{\frac{2}{\beta t}}\int_0^{\infty} dx \frac{\sin^2 x}{x^2}\sqrt{x} = \frac{\alpha^2}{4\sqrt{\beta}}\sqrt{t}.$$

(b) $\beta t \gg 1$: we set the lower limit in the integral equal to $-\infty$ and use the approximation $\sqrt{(2x/\beta t)+1} \simeq 1$ to obtain

$$S(t) \simeq \frac{\alpha^2\sqrt{2\pi}}{8\pi}t\int_{-\infty}^{\infty} dx \frac{\sin^2 x}{x^2} = \frac{\alpha^2\sqrt{2\pi}}{8}t.$$

Let us discuss the validity of the above result. Notice that we introduced approximations describing two-body interactions by contact potentials (renormalized δ-function potential). On the other hand, any realistic potential should have a natural ultraviolet cutoff k_c. If we extend the upper limit only up to k_c (instead of extending it to ∞), we find in the case (a) discussed above a narrow window of very short times when the number of scattered atoms grows quadratically in time. On later times, the dynamics will not be affected by the cutoff. Consequently, the realistic estimate would predict that the number of scattered atoms should be a quadratic function of time for an initial extremely short period, next there is a window of time when it behaves like a square root, and finally it turns into linear, semiclassical, regime.

E. Higher-order correlation functions

A lot of interesting information about the quantum systems might be obtained from its correlation functions. In this section, we present and discuss some of their properties. We focus on equal-time correlation functions in momentum space. This choice is justified by the fact that in most experiments performed with Bose-Einstein condensates, the common imaging technique is time-of-flight absorption, which directly registers the momentum distribution of the atomic cloud.

The normalized nth-order density correlation function ($n \geqslant 2$) is defined as

$$g_n(\mathbf{k}_1,\ldots,\mathbf{k}_n,t) = \frac{\langle \delta^\dagger(\mathbf{k}_1,t)\cdots\delta^\dagger(\mathbf{k}_n,t)\delta(\mathbf{k}_n,t)\cdots\delta(\mathbf{k}_1,t)\rangle}{\langle \delta^\dagger(\mathbf{k}_1,t)\delta(\mathbf{k}_1,t)\rangle\cdots\langle \delta^\dagger(\mathbf{k}_n,t)\delta(\mathbf{k}_n,t)\rangle}. \tag{36}$$

We make use of the fact that the evolution of $\hat{\delta}$ is linear, which means that $\hat{\delta}(\mathbf{k},t)$ is a linear combination of operators $\hat{\delta}(\mathbf{k}',0)$ and $\hat{\delta}^\dagger(\mathbf{k}',0)$; hence,

$$\hat{\delta}(\mathbf{k},t) = \int d\mathbf{k}'[U(\mathbf{k},\mathbf{k}',t)\hat{\delta}(\mathbf{k}',0) + V(\mathbf{k},\mathbf{k}',t)\hat{\delta}^\dagger(\mathbf{k}',0)].$$

For such a system, Wick's theorem applies. Since the averages are calculated in the vacuum state $|\Omega\rangle$, where $\hat{\delta}(\mathbf{k},0)|\Omega\rangle=0$ for all $\mathbf{k}$, all correlation functions decompose into a combination of products of a density matrix $\rho(\mathbf{k}_i,\mathbf{k}_j,t)$ and anomalous density $m(\mathbf{k}_l,\mathbf{k}_m,t)$, defined as

$$m(\mathbf{k}_1,\mathbf{k}_2,t) = \langle \hat{\delta}(\mathbf{k}_1,t)\hat{\delta}(\mathbf{k}_2,t)\rangle. \tag{37}$$

This leads to the growing complexity of the correlation functions, since in the nth order, the number of terms contributing to the g_n is of the order of $(2n-1)!!$. For example, the second-order correlation function

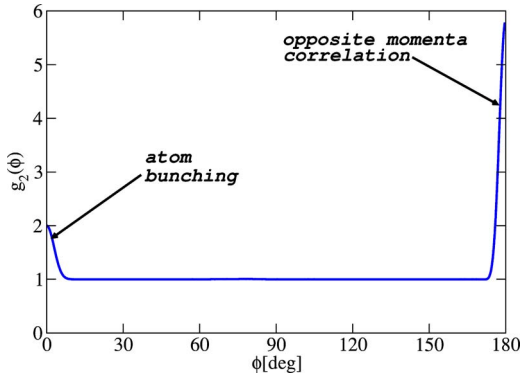

FIG. 9. (Color online) The second-order correlation function for $k_1=k_2=1$ as a function ϕ – relative angle between the vectors and $\alpha=20$, $\beta=30$. The strong maximum around $\phi=0$ corresponds to atom bunching. The maximum around $\phi=180°$ is an effect of correlations of pairs of atoms with opposite momenta.

$$g_2(\mathbf{k}_1,\mathbf{k}_2,t)=\frac{\langle\hat{\delta}^\dagger(\mathbf{k}_1,t)\hat{\delta}^\dagger(\mathbf{k}_2,t)\hat{\delta}(\mathbf{k}_2,t)\hat{\delta}(\mathbf{k}_1,t)\rangle}{\langle\delta^\dagger(\mathbf{k}_1,t)\hat{\delta}(\mathbf{k}_1,t)\rangle\langle\hat{\delta}^\dagger(\mathbf{k}_2,t)\hat{\delta}(\mathbf{k}_2,t)\rangle}$$

takes the form

$$g_2(\mathbf{k}_1,\mathbf{k}_2,t)=1+\frac{|\rho(\mathbf{k}_1,\mathbf{k}_2,t)|^2+|m(\mathbf{k}_1,\mathbf{k}_2,t)|^2}{\rho(\mathbf{k}_1,\mathbf{k}_1,t)\rho(\mathbf{k}_2,\mathbf{k}_2,t)}. \quad (38)$$

In the first order, we find an analytical expression for the anomalous density,

$$\begin{aligned}m(\mathbf{k}_1,\mathbf{k}_2,t)&=-i\frac{\alpha\beta^2}{8\pi^{3/2}}\exp\left(-\frac{\beta^2(\mathbf{k}_1+\mathbf{k}_2)^2}{4}\right)\int_0^t d\tau\\&\times\exp\left[-\tau^2-i\beta\tau\left(1-\frac{k_1^2+k_2^2}{2}\right)\right]\\&=-i\frac{\alpha\beta^2}{16\pi}\exp\left[-\frac{\beta^2(\mathbf{k}_1+\mathbf{k}_2)^2}{4}\right.\\&\left.-\frac{\beta^2}{4}\left(1-\frac{k_1^2+k_2^2}{2}\right)^2\right]\\&\times\left\{\mathrm{erf}\left[t+\frac{i}{2}\beta\left(1-\frac{k_1^2+k_2^2}{2}\right)\right]\right.\\&\left.-\mathrm{erf}\left[\frac{i}{2}\beta\left(1-\frac{k_1^2+k_2^2}{2}\right)\right]\right\}. \quad (39)\end{aligned}$$

The above function reaches its maximum when $\mathbf{k}_1=-\mathbf{k}_2$ and both vectors are of unit length ($k_1=k_2=1$) due to the energy and momentum conservation.

Combining Eqs. (38) and (39) with the expressions for the density matrix discussed before, we can find an analytic expression for the second-order correlation function in the first-order perturbation theory. In Fig. 9, we show the second-order correlation function for $k_1=k_2=1$ as a function of relative angle ϕ between the vectors. The maximum around $\phi=0$ corresponds to the detection of two scattered particles close to each other. It is greater than 1 due to the bosonic statistics of scattered atoms. This effect is called *atom bunching*. Since the atoms scatter in pairs of opposite momenta, the g_2 correlation function reveals strong correlation around $\phi=180°$. It is exclusively an anomalous density part of the second-order correlation function that contributes to this maximum.

IV. CONCLUSIONS

We studied the nature of the transition from the spontaneous to the stimulated scattering regime in the collision of two Bose-Einstein condensates. Within the first-order approximation, we derived analytical expressions for the density matrix and anomalous density. This enabled us to derive the condition for the bosonic stimulation effect. The characteristic time scales in the dynamics of scattered atoms were identified. Finally, we showed that scattered atoms feature both bunching as well as the opposite momenta correlations.

ACKNOWLEDGMENTS

The authors would like to acknowledge support from KBN Grant Nos. GR-2244 (P.Z.), GR-2242 (J.C.), and the Polish Ministry of Scientific Research and Information Technology under Grant No. PBZ-MIN-008/P03/2003 (M.T.). Special thanks are due to Professor Kazimierz Rzążewski for valuable and stimulating discussions and to Baltazar Brukalski for creating the artistic view presented in Fig. 6.

APPENDIX A

In this appendix, we simplify the expression for density matrix (22) upon evaluating the integral over d^3k in the limit $\beta\gg1$. The angular part of this integral can be performed analytically,

$$\begin{aligned}&\int d^3k\exp\left(-\frac{\beta^2[k^2+\mathbf{k}\cdot(\mathbf{k}_1+\mathbf{k}_2)]}{2}\right)\\&\times\exp\left[i\beta(\tau-\tau')\left(1-\frac{k^2}{2}\right)\right]\\&=2\pi\int_0^\infty k^2dk\frac{4}{\beta^2|\mathbf{k}_1+\mathbf{k}_2|k}\sinh\left(\frac{\beta^2k|\mathbf{k}_1+\mathbf{k}_2|}{2}\right)\\&\times\exp\left[-\frac{\beta^2k^2}{2}+i\beta(\tau-\tau')\left(1-\frac{k^2}{2}\right)\right].\end{aligned}$$

Next, using the identity $2(k_1^2+k_2^2)=|\mathbf{k}_1+\mathbf{k}_2|^2+|\mathbf{k}_1-\mathbf{k}_2|^2$, we get

$$\begin{aligned}\rho(\mathbf{k}_1,\mathbf{k}_2,t)&=\frac{\alpha^2\beta^2}{16\pi^2}\frac{1}{|\mathbf{k}_1+\mathbf{k}_2|}\exp\left(-\frac{\beta^2|\mathbf{k}_1-\mathbf{k}_2|^2}{8}\right)\int_0^t d\tau\int_0^t d\tau'\\&\times\exp[-\tau^2-\tau'^2-i\beta(\tau k_1^2-\tau' k_2^2)/2+i\beta(\tau-\tau')]\\&\times\int_0^\infty kdk\exp\left(-i\frac{\beta}{2}(\tau-\tau')k^2\right)\\&\times\left\{\exp\left[-\frac{\beta^2}{2}\left(k-\frac{|\mathbf{k}_1+\mathbf{k}_2|}{2}\right)^2\right]\right.\\&\left.-\exp\left[-\frac{\beta^2}{2}\left(k+\frac{|\mathbf{k}_1+\mathbf{k}_2|}{2}\right)^2\right]\right\}. \quad (A1)\end{aligned}$$

The most significant contribution to the above integral comes from the region where the condition $\beta|\mathbf{k}_1+\mathbf{k}_2| \gg 1$ is satisfied. In this region, we can neglect

$$\exp\left[-\frac{\beta^2}{2}\left(k+\frac{|\mathbf{k}_1+\mathbf{k}_2|}{2}\right)^2\right]$$

in comparison with

$$\exp\left[-\frac{\beta^2}{2}\left(k-\frac{|\mathbf{k}_1+\mathbf{k}_2|}{2}\right)^2\right].$$

Additionally, we introduce a new variable $k=(|\mathbf{k}_1+\mathbf{k}_2|/2)+(x/\beta)$ and get

$$\begin{aligned}\int_0^\infty kdk\exp\left(-i\frac{\beta}{2}(\tau-\tau')k^2\right)&\exp\left[-\frac{\beta^2}{2}\left(k-\frac{|\mathbf{k}_1+\mathbf{k}_2|}{2}\right)^2\right]\\ &=\frac{1}{\beta^2}\int_{-\beta|\mathbf{k}_1+\mathbf{k}_2|/2}^\infty dx(\beta|\mathbf{k}_1+\mathbf{k}_2|/2+x)\\ &\times\exp\left[-\frac{i}{8}(\tau-\tau')\left(\beta|\mathbf{k}_1+\mathbf{k}_2|^2+4x|\mathbf{k}_1+\mathbf{k}_2|+\frac{4x^2}{\beta}\right)\right]\\ &\times\exp(-x^2/2).\end{aligned} \tag{A2}$$

The condition $\beta|\mathbf{k}_1+\mathbf{k}_2| \gg 1$, together with the presence of the exponential factor $\exp(-x^2/2)$, allow us to extend the lower limit in the integral over x in Eq. (A2) to $-\infty$, and neglect x in comparison with $\beta|\mathbf{k}_1+\mathbf{k}_2|/2$. Due to the presence of the exponential factor $\exp(-\tau^2-\tau'^2)$ in Eq. (A1), we can make another approximation, namely neglect the phase factor $i(\tau-\tau')(x^2/2\beta)$. Having all the above approximation applied, we can evaluate the simple Gaussian integral to get finally

$$\begin{aligned}\rho(\mathbf{k}_1,\mathbf{k}_2,t)=\frac{\alpha^2\beta\sqrt{2\pi}}{32\pi^2}&\exp\left(-\frac{\beta^2|\mathbf{k}_1-\mathbf{k}_2|^2}{8}\right)\int_0^t d\tau\int_0^t d\tau'\\ &\times\exp\left(-\tau^2-\tau'^2-\frac{(\tau-\tau')^2|\mathbf{k}_1+\mathbf{k}_2|^2}{8}\right)\\ &\times\exp\left[i\beta\tau\left(1-\frac{|\mathbf{k}_1+\mathbf{k}_2|^2}{8}-\frac{k_1^2}{2}\right)\right.\\ &\left.-i\beta\tau'\left(1-\frac{|\mathbf{k}_1+\mathbf{k}_2|^2}{8}-\frac{k_2^2}{2}\right)\right].\end{aligned} \tag{A3}$$

APPENDIX B

In this appendix, we calculate the collisional loss for two counterpropagating clouds of classical particles. This model is meant as a classical counterpart of the collision described in the main body of the paper. To match the conditions used in the paper, we assume a Gaussian density profile for each of the clouds and we restrict ourselves to the dilute gas limit ($n\sigma_0\sigma \ll 1$), where σ_0 is a cross section for a collision of two particles and σ is the radius of the cloud. In this limit, we neglect secondary collisions. We also ignore the depletion of the clouds; this approximation is valid as long as the fraction of scattered atoms is small. When the collision is described in the reference frame associated with one of the clouds, the density of this cloud is equal to

$$n_1(\mathbf{r})=\frac{N}{2\pi^{3/2}\sigma^3}\exp\left[-\frac{x_1^2+x_2^2+x_3^2}{\sigma^2}\right],$$

while the other cloud propagates along the x_1 axis with velocity $2v$,

$$n_2(\mathbf{r},t)=\frac{N}{2\pi^{3/2}\sigma^3}\exp\left[-\frac{(x_1+2vt)^2+x_2^2+x_3^2}{\sigma^2}\right].$$

Here both clouds contain $N/2$ particles.

The number of particles scattered up to the time t equals

$$\mathcal{S}(t)=2\left[\int d^3r n_1(\mathbf{r})\int_0^t dt'[n_2(\mathbf{r},t')\cdot 2v\sigma_0]\right].$$

Here, the prefactor "2" on the right-hand side accounts for the fact that in every collision two particles are scattered. For two identical bosons, the cross section σ_0 at the low-energy limit is equal to $8\pi a^2$, where a is the s-wave scattering length. Using the identity

$$\int_{-\infty}^\infty\exp\left(-\frac{x^2}{\sigma^2}\right)\mathrm{erf}\left(\frac{x+2vt}{\sigma}\right)dx=\sqrt{\pi}\sigma\,\mathrm{erf}\left(\frac{\sqrt{2}vt}{\sigma}\right)$$

and rescaling time ($t/t_C \to t$), where the collisional time $t_C=\sigma/v$, we obtain

$$\mathcal{S}(t)=\frac{N^2a^2}{\sigma^2}\,\mathrm{erf}(t\sqrt{2})=\frac{\alpha^2\pi}{16}\,\mathrm{erf}(t\sqrt{2}).$$

This result reproduces the number of scattered atoms obtained in the quantum model within the first-order perturbation theory [16].

[1] Yu. B. Ovchinnikov *et al.*, Phys. Rev. Lett. **83**, 284 (1999).
[2] M. Kozuma *et al.*, Phys. Rev. Lett. **82**, 871 (1999).
[3] J. Stenger *et al.*, Phys. Rev. Lett. **82**, 4569 (1999).
[4] E. W. Hagley *et al.*, Science **283**, 1706 (1999).
[5] E. W. Hagley *et al.*, Phys. Rev. Lett. **83**, 3112 (1999).
[6] M. Trippenbach *et al.*, J. Phys. B **33**, 47 (2000).
[7] G. Lenz, P. Meystre, and E. M. Wright, Phys. Rev. Lett. **71**, 3271 (1993); E. Goldstein, K. Plattner, and P. Meystre, Quantum Semiclassic. Opt. **7**, 743 (1995); E. Goldstein, K. Plattner, and P. Meystre, J. Res. Natl. Inst. Stand. Technol. **101**, 583 (1996); E. Goldstein and P. Meystre, Phys. Rev. A **59**, 1509 (1999).
[8] M. Trippenbach, Y. B. Band, and P. S. Julienne, Opt. Express **3**, 530 (1998).
[9] M. Trippenbach, Y. B. Band, and P. S. Julienne, Phys. Rev. A **62**, 023608 (2000).

[10] L. Deng *et al.*, Nature (London) **398**, 218 (1999).
[11] J. M. Vogels, K. Xu, and W. Ketterle, Phys. Rev. Lett. **89**, 020401 (2002).
[12] N. Katz, R. Ozeri, E. Rowen, E. Gershnabel, and N. Davidson, Phys. Rev. A **70**, 033615 (2004); N. Katz, E. Rowen, R. Ozeri, and N. Davidson, e-print cond-mat/0505762.
[13] Y. B. Band *et al.*, Phys. Rev. Lett. **84**, 5462 (2000).
[14] J. Chwedeńczuk, M. Trippenbach, and K. Rzążewski, J. Phys. B **37**, L391 (2004).
[15] A. A. Norrie, R. J. Ballagh, and C. W. Gardiner, Phys. Rev. Lett. **94**, 040401 (2005); see also A. Sinatra, Y. Castin, and C. Lobo, J. Mod. Opt. **47**, 2629 (2000).
[16] R. Bach, M. Trippenbach, and K. Rzążewski, Phys. Rev. A **65**, 063605 (2002).
[17] V. A. Yurovsky, Phys. Rev. A **65**, 033605 (2002).
[18] P. Ziń *et al.*, Phys. Rev. Lett. **94**, 200401 (2005).
[19] Y. Castin and R. Dum, Phys. Rev. Lett. **77**, 5315 (1996); Yu. Kagan, E. L. Surkov, and G. V. Shlyapnikov, Phys. Rev. A **55**, R18 (1997).
[20] M. Abramovich and I. A. Stegun, *Handbook of Mathematical Functions with Formulas, Graphs and Mathematical Tables* (Dover Publications, New York, 1974).
[21] R. P. Feynman, *Feynman Lectures on Physics* (Addison Wesley Longman, Reading, MA, 1970), Vol. 3.